

# Photophysics of $\alpha,\omega$ -Diphenyloctatetraene in the Vapor Phase

Takao Itoh\*

Graduate School of Integrated Arts and Sciences, Hiroshima University, 1-7-1 Kagamiyama, Higashi-Hiroshima City, 739-8521 Japan

Received: July 12, 2006; In Final Form: December 10, 2006

Fluorescence and fluorescence excitation spectra of diphenyloctatetraene vapor have been measured at different temperatures from 98 to 136 °C and at different buffer gas pressures from 0 to 300 Torr. The fluorescence quantum yields were determined as functions of the excitation energy and buffer gas pressure. It is shown that diphenyloctatetraene vapor exhibits weak fluorescence from the  $S_2$  ( $1^1\text{Bu}$ ) state in addition to the fluorescence from the  $S_1$  ( $2^1\text{Ag}$ ) state. The quantum yield of the  $S_1$  fluorescence is shown to decrease with decreasing pressure and with increasing excitation energy. The electronic relaxation processes of diphenyloctatetraene vapor are discussed based on the pressure and excitation-energy dependence of the fluorescence quantum yield.

## 1. Introduction

Diphenylpolyenes have been the subject of a number of spectroscopic investigations because such studies advance our understanding of polyene electronic structure and the connection between that structure and photophysical property.<sup>1–29</sup> Diphenyloctatetraene (DPO) is a typical polyene that led to the discovery of the low-lying one-photon forbidden  $2^1\text{Ag}$  state of linear polyenes.<sup>1–3</sup> It is now well-established for diphenylpolyene vapors with a polyene double-bond number from 2 to 4 that the lowest-energy excited singlet state,  $S_1$ , is  $2^1\text{Ag}$  and that the  $1^1\text{Bu}$  state is the second excited state,  $S_2$ .<sup>4–10</sup> To obtain deeper insight into the photophysical processes of diphenylpolyenes, it is essential to investigate the emission property in the vapor phase where the molecule suffers no interaction from the environment.

We tried to measure the emission and excitation spectrum of DPO in a supersonic jet expansion in the past.<sup>4,5</sup> Unfortunately, however, we could not detect any emission signals in a jet, although the emission signals could be detected for diphenylbutadiene and diphenylhexatriene vapors in a jet.<sup>4,6,7</sup> This is presumably due to the low vapor pressure and low fluorescence quantum yield of DPO as compared with those of diphenylbutadiene and diphenylhexatriene. However, the techniques of photon counting combined with electric cooling of the photomultiplier and the use of a double monochromator enable us to measure the weak emission signals from the static vapor.

It is reported that diphenylhexatriene and DPO vapors exhibit the fluorescence solely from the  $S_1$  state. However, diphenylpolyenes with the polyene double-bond number ( $n$ ) over five are known to show the  $S_2$  ( $1^1\text{Bu}$ ) fluorescence, the relative fluorescence yield of which tends to increase with increasing polyene chain length or  $S_1 - S_2$  energy separation: In solution, diphenyldecapentaene ( $n = 5$ ), diphenyldodecahexaene ( $n = 6$ ), and diphenyltetradecaheptaene ( $n = 7$ ) exhibit the  $S_2$  ( $1^1\text{Bu}$ ) fluorescence, the relative intensity of which increases significantly with increasing polyene chain length.<sup>28,29</sup> This observation has been interpreted in terms of the energy gap law and intensity borrowing of  $S_1$  from  $S_2$ .<sup>28–30</sup> Furthermore, in contrast to the case of DPO vapor, the major emission of unsubstituted

octatetraene and methyl-substituted octatetraene vapors consists of the  $S_2$  fluorescence.<sup>31</sup> The striking difference between DPO vapor and unsubstituted or methyl-substituted octatetraene vapor also poses some fundamental questions concerning the relaxation processes of polyene excited states as well as the mechanism of the occurrence of the  $S_2$  fluorescence. It is, therefore, of interest to see whether or not the DPO shows the  $S_2$  fluorescence in addition to the  $S_1$  fluorescence in the vapor phase, where the  $S_1 - S_2$  energy difference is much larger than that in solution as well as that of diphenylhexatriene vapor. In addition, the detailed information on the relaxation processes in the  $S_1$  manifold is not available for DPO vapor.

In the present work, we have measured the fluorescence and fluorescence excitation spectra of DPO in the static vapor phase at temperatures from 98 to 136 °C at different buffer gas pressures from 0 up to 300 Torr. It is shown that DPO exhibits the detectable weak fluorescence from the  $S_2$  ( $1^1\text{Bu}$ ) state in addition to the fluorescence from the  $S_1$  ( $2^1\text{Ag}$ ) state. Furthermore, the fluorescence spectra measured at different excitation energies and pressures as well as the excitation spectra revealed that the  $S_1$  fluorescence quantum yield decreases with decreasing pressure and with increasing excitation energy. The electronic relaxation processes of DPO vapor have been discussed based on the obtained data.

## 2. Experimental Section

**2.1. Sample Preparation.** Diphenyloctatetraene (DPO) obtained from Aldrich was purified by repeated recrystallization from hexane. No impurity emission was detected when the purified sample was dissolved in *n*-pentane and measured with a fluorimeter. The perfluorohexane obtained from Aldrich was used as a buffer gas without purification, after we confirmed that it contained no impurities that emitted under the condition of our experiments. Samples were prepared on an all-glass made vacuum line equipped with a diffusion pump. Perfluorohexane sealed in a side arm was degassed by repeated freeze–pump–thaw cycles. A small amount of DPO crystal in a nonfluorescent 10-mm square quartz cell sealed to the vacuum system was heated to 80 °C at a background pressure of less than  $10^{-4}$  Torr in order to remove volatile impurities such as water. Buffer gas

\* E-mail: titoh@hiroshima-u.ac.jp.

was admitted into the sample cell after degassing. The pressure of the buffer gas was controlled by the temperature of the side arm varied from  $-25$  to  $-5$  °C. The sample cell with buffer gas was then isolated from the buffer gas reservoir, the contents were trapped by liquid nitrogen, and the cell was sealed off. By measuring the pressure and volume of the buffer gas before trapping and by measuring the volume of the cell at the end of the experiment, we estimated the buffer gas pressure.

**2.2. Measurements.** The emission and excitation spectra were measured with a Spex Fluorolog-3 (Model 21-SS) spectrophotometer equipped with a double-grating excitation monochromator, a high-pressure 450-W Xenon lamp as an excitation-light source, and a photomultiplier tube (Hamamatsu R928-P) in an electric-cooled housing operated in photon-counting mode. For most of the emission measurement, square 10-mm path length quartz cells were used. Absorption spectra were measured with a Shimadzu UV-2550 spectrophotometer, with which the optical densities as low as 0.003 can be measured with a reasonable  $S/N$  ratio. The absorption spectrum of the vapor sample was measured using a cylindrical 100-mm path length quartz cell at 150 °C. The temperature of the sample cells was controlled by thermostated cell holders. In the emission measurements, the temperature of the lower portion of the cell was always kept higher than that of the upper portion by 5–10 °C and was measured with a digital thermometer. Background and scattered light were subtracted from the measured spectra. Fluorescence spectra were corrected for the spectral sensitivity of the detection system determined by using quinine in sulfuric acid as a standard. Excitation spectra were corrected for the spectral intensity distribution of the exciting light with an aqueous solution of rhodamine B as a quantum counter. Emission quantum yields were determined by comparing the corrected emission spectra of the samples with that of quinine in sulfuric acid used as a standard, which is assumed to have a fluorescence quantum yield of 0.51. However, determination of the accurate value of the fluorescence quantum yield accompanied some difficulties, primarily because of the extremely low optical density and the low emission intensity of DPO vapor. The fluorescence quantum yield of DPO vapor was determined to be approximately 0.1 for the excitation at near the  $S_2$  origin in the presence of 310 Torr perfluorohaxane at 130 °C.

### 3. Results and Discussion

Figure 1 shows absorption, fluorescence, and fluorescence excitation spectra of DPO vapor in the presence of 290 Torr perfluorohexane. It is seen that most of the emission consists of the fluorescence from the  $S_1$  ( $2^1Ag$ ) state, as has been reported previously.<sup>5</sup> Closer inspection reveals a very weak emission band observed near 400 nm ( $25\,000\text{ cm}^{-1}$ ) beside the comparatively strong  $S_1$  ( $2^1Ag$ ) fluorescence. This weak emission is assigned to the  $S_2$  ( $1^1Bu$ ) fluorescence based on the following observations: (1) the structure of the excitation spectrum obtained by monitoring only the apparent origin band region of the  $S_2$  fluorescence corresponds nearly to that of the absorption spectrum; (2) the reflected  $S_0 - S_2$  absorption spectrum matches the high-energy band of the observed fluorescence, which can be assigned to the apparent  $S_2$  fluorescence origin: Furthermore, closer inspection of Figure 1 shows that there is also a weak emission band seen at  $24\,800\text{ cm}^{-1}$ , which can be attributed to the second vibronic band of the  $S_2$  fluorescence forming the mirror-image relation to the second  $S_0 \rightarrow S_2$  absorption band at about  $29\,500\text{ cm}^{-1}$ .

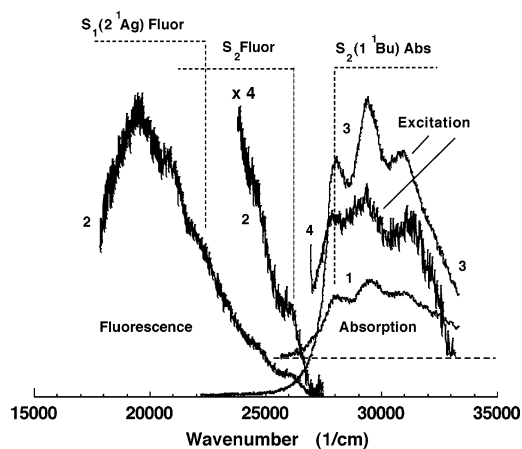


**Figure 1.** Absorption (1), corrected fluorescence (2), and corrected fluorescence excitation spectra (3 and 4) of DPO vapor in the presence of 290 Torr perfluorohexane. The fluorescence spectrum 2 was obtained by excitation at 350 nm, and the excitation spectra 3 and 4 were obtained by monitoring the emission at 500 and at 385 nm, respectively. The baseline of the absorption spectrum is shown by a broken line.

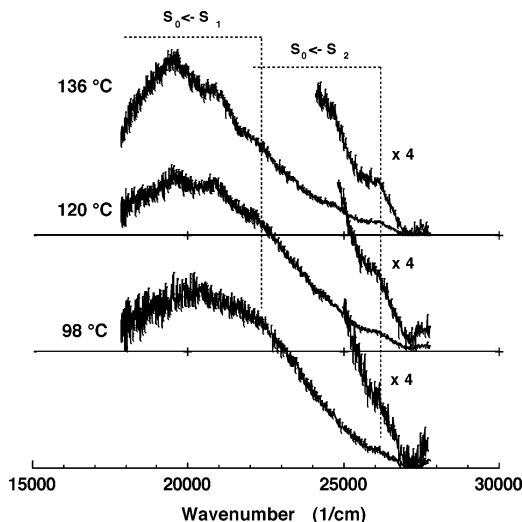


**Figure 2.** Corrected fluorescence spectra of DPO vapor in the presence of 290 Torr perfluorohexane obtained by excitation at 340 nm at different temperatures.

**3.1. Temperature Dependence of the Fluorescence Spectrum.** Figure 2 shows the fluorescence spectra of DPO vapor at high total pressure at different temperatures. Because of the extremely low intensity of the  $S_2$  fluorescence, we could not carry out the quantitative analysis of the intensity. However, the spectra in Figure 2 show vaguely that the relative intensity of the  $S_2$  fluorescence to the  $S_1$  fluorescence increases slightly with increasing temperature. If the whole intensity of the  $S_2$  fluorescence was originating entirely from the thermal population of the  $S_1$  state, then the intensity ratio of the  $S_2$  to  $S_1$  fluorescence,  $I_{F2}/I_{F1}$ , at temperature,  $T$ , should be proportional to the value  $k_{F2}/k_{F1} \times \exp(-\Delta E_{12}/kT)$ , with  $k_{F1}$ ,  $k_{F2}$ ,  $\Delta E_{12}$ , and  $k$  denoting the radiative rate constant of the  $S_1$  and  $S_2$  states, the energy difference between the  $S_1$  and  $S_2$  states, and the Boltzmann constant, respectively. The value for  $\Delta E_{12}$  is estimated to be about  $4000\text{ cm}^{-1}$  for DPO vapor, based on the energy difference between the observed  $S_1$  and  $S_2$  fluorescence origins:<sup>32</sup> The  $S_1$  fluorescence origin of DPO vapor has been observed at  $22020 \pm 23\text{ cm}^{-1}$ , while the  $S_2$  fluorescence origin is seen at  $26\,100\text{ cm}^{-1}$  (see Figure 1). The “ratio” of the  $S_2/S_1$

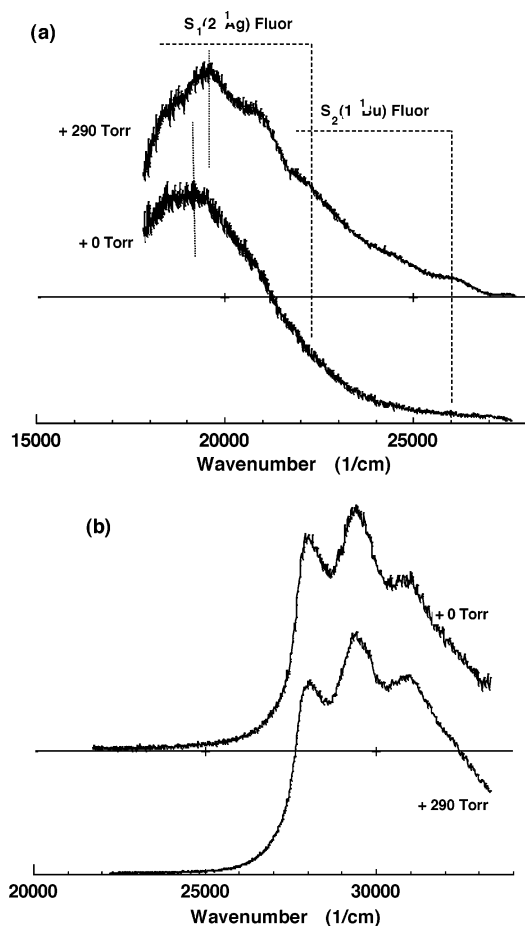


**Figure 3.** Corrected fluorescence (a) and fluorescence excitation spectra (b) of DPO vapor in the presence and absence of perfluorohexane at 134 °C. The fluorescence spectrum was obtained by excitation at 345 nm, and the excitation spectrum was obtained by monitoring the emission at 500 nm.

fluorescence intensity ratio,  $I_{F2}/I_{F1}$ , at two different temperatures,  $T_1$  and  $T_2$ , is given by

$$\left[\frac{I_{F2}/I_{F1}}{T=T_1}\right] / \left[\frac{I_{F2}/I_{F1}}{T=T_2}\right] = \exp\left[\frac{\Delta E_{12}}{k} \times \left(\frac{1}{T_2} - \frac{1}{T_1}\right)\right] \quad (1)$$

Assuming that the  $\Delta E_{12}$  value is  $4000 \text{ cm}^{-1}$ , the ratio expressed by the above equation with  $T_1 = 98 \text{ °C}$  and  $T_2 = 136 \text{ °C}$  is calculated to be 4.2. As is seen in Figure 2, the origin band intensity of the  $S_2$  fluorescence does not exhibit such a large increase with increasing temperature from 98 to 136 °C. This indicates that all of the intensity of the  $S_2$  fluorescence does not originate from the Boltzmann distribution of the  $S_1$  state. A part of the observed  $S_2$  fluorescence presumably involves the contribution from the prompt fluorescence originating directly from the  $S_2$  state.

**3.2. Pressure and Excitation Energy Dependence of the Fluorescence Spectrum and Quantum Yield.** Figure 3a shows the fluorescence spectra of DPO vapor in the presence and absence of the buffer gas. At low pressure without the buffer gas, the fluorescence spectrum is broad and tends to shift to the red as compared with that at high total pressure, while the fluorescence is somewhat structured in the presence of the buffer gas. This observation indicates that at low pressure the fluorescence originates from the unrelaxed vibrational levels in the  $S_1$  state, whereas at high total pressure the fluorescence originates from the relaxed levels near the  $S_1$  origin. The  $S_2$  fluorescence tends to be weakened at low pressure, but this is

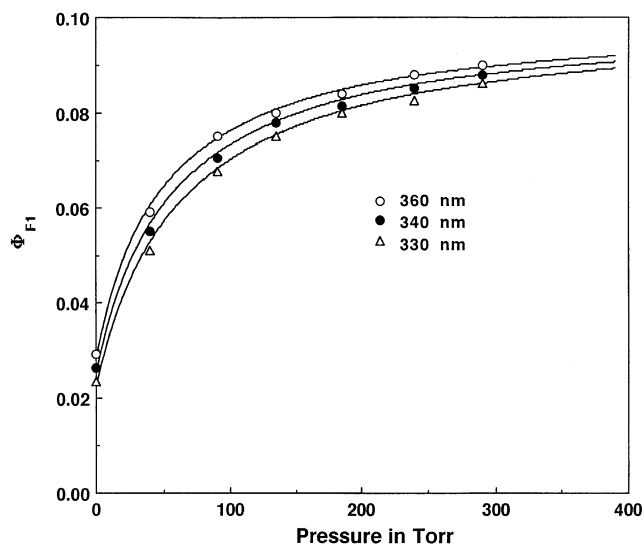


**Figure 4.** Pressure dependence of the  $S_1$  fluorescence quantum yield obtained by the excitation at different wavelengths at 134 °C. The solid curves are the best-fitted ones.

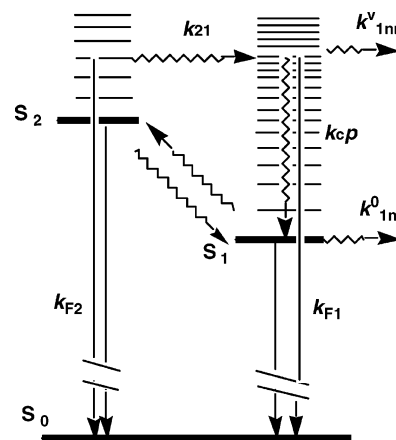


**Figure 5.** Kinetic scheme for the electronic relaxation of DPO vapor.

presumably due to the broadness of the  $S_2$  and  $S_1$  fluorescence. In fact, the higher-energy tail of the  $S_1$  fluorescence is extended to near the  $S_2$  absorption origin, and the  $S_2$  fluorescence could be hidden in part by the long tail of the  $S_1$  fluorescence. Figure 3b shows the excitation spectra of DPO vapor in the presence and absence of the buffer gas. It is seen that at low pressure the intensity decreases with increasing excitation energy as compared with that at high total pressure. The  $S_1$ -fluorescence quantum yield plotted against the buffer gas pressure is shown in Figure 4 for different excitation energies, where the yield decreases with decreasing buffer gas pressure and with increasing excitation energy. Although DPO vapor was shown to emit a weak  $S_2$  fluorescence, the detailed analysis could not be made for the pressure dependence of the quantum yield because of the weakness of the emission intensity.

The observed pressure and excitation energy dependence of the population of the  $S_1$  ( $2^1A_g$ ) state can be accounted for in a relaxation scheme as shown in Figure 5, which involves the collisional deactivation in the  $S_1$  state. In the limit of low pressure without the buffer gas, the DPO molecule can be safely regarded as collision-free during the lifetime of the excited states because the vapor pressure of pure DPO is estimated to be around 2 mTorr at temperatures used in the present experiment. At 2 mTorr, the collision interval is estimated to be approximately  $5 \times 10^{-5} \text{ s}$ , while the intrinsic fluorescence lifetime of the  $S_1$  state obtained from the measured fluorescence decay

time and quantum yield in cyclohexane at room temperature is 70 ns.<sup>2,9,33</sup> Alternatively, in the limit of high pressure there were sufficient collisions during the lifetime of the  $S_1$  state to bring about collisional deactivation to lower vibrational levels of the  $S_1$  state so that the photophysical behavior is similar to that observed in the condensed phase. Thus, at high total pressure the fluorescence spectrum exhibits some structure, whereas at low pressure the spectrum is broad.

In the kinetic scheme shown in Figure 5, the  $S_1$ -fluorescence quantum yield,  $\Phi_{F1}$ , at a particular pressure,  $p$ , of the buffer gas is given by

$$\Phi_{F1} = [k_{21}/(k_{F2} + k_{21})] \times [1 + k_c p / (k_{F1} + k_{1nr}^0)] \times [k_{F1}/(k_{F1} + k_c p + k_{1nr}^v)] \quad (2)$$

where  $k_{1nr}^0$  and  $k_{1nr}^v$  are, respectively, the rate constants for nonradiative decay from the levels in the neighborhood of the  $S_1$  origin and the vibrationally excited levels in  $S_1$ , and  $k_c$  is the rate constant for collisional deactivation in the  $S_1$  manifold. The nonradiative pass from the  $S_1$  state possibly includes the isomerization process. The values for  $\Phi_{F1}$  plotted as a function of  $p$  shown in Figure 4 are well fit by this model. Because the intrinsic fluorescence lifetime of the  $S_1$  state is about 70 ns, the value for  $k_{F1}$  is evaluated to be  $1.4 \times 10^7 \text{ s}^{-1}$ . With the assumption that  $k_c = 1 \times 10^7 \text{ Torr}^{-1} \text{ s}^{-1}$ , the data in Figure 4 provide  $k_{1nr}^v = 4.8 \times 10^8$ ,  $5.4 \times 10^8$ , and  $6.1 \times 10^8 \text{ s}^{-1}$ , respectively, for 360, 340, and 330 nm excitations. It follows from eq 2 that at zero pressure  $1/\Phi_{F1}$  is given by

$$1/\Phi_{F1} = (1 + k_{F2}/k_{21}) \times (1 + k_{1nr}^v/k_{F1}) \quad (3)$$

Because  $k_{F1} \ll k_{1nr}^v$  and  $k_{F2} \ll k_{21}$ , we have to a good approximation  $1/\Phi_{F1} \sim k_{1nr}^v/k_{F1}$ . By division of the fluorescence excitation spectrum measured at high total pressure by the fluorescence excitation spectrum measured with no buffer gas, the excitation energy dependence of  $1/\Phi_{F1}$  and, hence, the excitation energy dependence of  $k_{1nr}^v$  may be directly seen because the excitation spectrum at high total pressure is to a good approximation regarded as the absorption spectrum. Clearly,  $1/\Phi_{F1}$  or, equivalently,  $k_{1nr}^v/k_{F1}$ , increases with excitation energy in good agreement with the excitation-energy dependence of  $k_{1nr}^v$  obtained from the pressure dependence of  $\Phi_{F1}$  (see Figure 4). Thus, the nonradiative rate from the  $S_1$  state increases with increasing excitation energy, but the increase is small compared to that observed for diphenylhexatriene or diphenylbutadiene vapor.<sup>5,10</sup> Furthermore, it is seen vaguely in Figure 6 that the relative fluorescence quantum yield undergoes an abrupt increase when the excitation energy is lowered to bring the DPO molecule into the  $S_1$  ( $2^1A_g$ ) state from  $S_2$  ( $1^1B_u$ ). A similar abrupt increase of the fluorescence yield has also been observed more clearly for diphenylbutadiene and diphenylhexatriene vapors.<sup>5,8</sup> It follows from these observations that there should be a mechanism that causes an abrupt increase in the fluorescence yield. This mechanism may possibly include the slow vibrational energy redistribution in the  $S_1$  state between the optical modes and the modes achieved by the  $S_2 \rightarrow S_1$  internal conversion.

#### 4. Conclusions

DPO vapor is shown to exhibit the weak fluorescence from the  $S_2$  ( $1^1B_u$ ) state in addition to the fluorescence from the  $S_1$  ( $2^1A_g$ ) state. The electronic relaxation processes of DPO vapor are revealed based on the pressure and excitation-energy dependence of the fluorescence quantum yield. The quantum

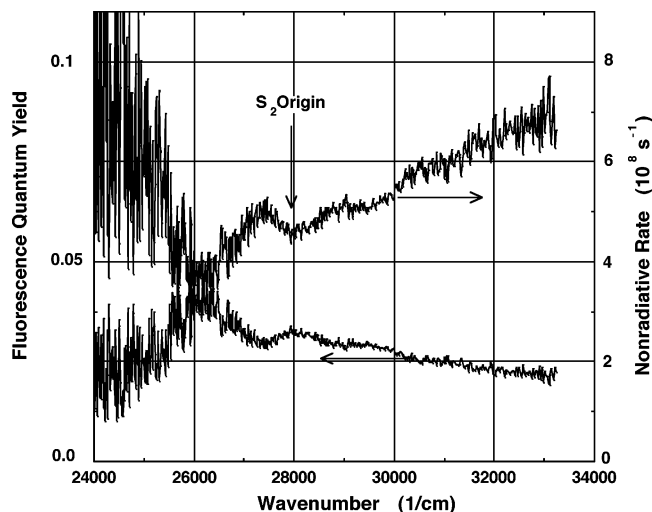


**Figure 6.** Fluorescence quantum yield (1) and the nonradiative rate from the  $S_1$  state (2) of pure DPO vapor plotted against the excitation energy.

yield of the  $S_1$  fluorescence is found to increase with increasing pressure and with decreasing excitation energy, indicating that the nonradiative rate from the  $S_1$  state increases with increasing excitation energy, although the decrease is small compared to that seen in the case of diphenylhexatriene or diphenylbutadiene vapor. It is indicated that the vibrational energy redistribution in the  $S_1$  state is slow as compared with other nonradiative processes including possible isomerization processes.

#### References and Notes

- (1) Hudson, B. S.; Kohler, B. E. *Chem. Phys. Lett.* **1972**, *14*, 299–304.
- (2) Hudson, B. S.; Kohler, B. E. *J. Chem. Phys.* **1973**, *59*, 4984–5002.
- (3) Hudson, B. S.; Kohler, B. E.; Schulten, K. *Excited States* **1982**, *5*, 1–95.
- (4) Horwitz, J. S.; Itoh, T.; Kohler, B. E.; Spiglanin, T. A. *SPIE* **1989**, *1057*, 72–81.
- (5) Itoh, T.; Kohler, B. E. *J. Phys. Chem.* **1988**, *92*, 1807–1813.
- (6) Heimbrook, L. A.; Kohler, B. E.; Spiglanin, T. A. *Proc. Natl. Acad. Sci. U.S.A.* **1983**, *80*, 4580–4584.
- (7) Kohler, B. E.; Spiglanin, T. A. *J. Chem. Phys.* **1984**, *80*, 5465–5471.
- (8) Amirav, A.; Sonnenschein, M.; Jortner, J. *Chem. Phys.* **1986**, *102*, 305–312.
- (9) Allen, M. T.; Whitten, D. G. *Chem. Rev.* **1989**, *89*, 1691–1702.
- (10) Shepanski, J. F.; Keelan, B. W.; Zewail, A. H. *Chem. Phys. Lett.* **1983**, *103*, 9–14.
- (11) Holtom, G. R.; McClain, W. M. *Chem. Phys. Lett.* **1976**, *44*, 436–439.
- (12) Fang, H. L. B.; Thrash, R. J.; Leroi, G. E. *J. Chem. Phys.* **1977**, *67*, 3389–3391.
- (13) Bachilo, S. M.; Gillbro, T. *Chem. Phys. Lett.* **1984**, *218*, 557–562.
- (14) Itoh, T.; Kohler, B. E. *J. Phys. Chem.* **1987**, *91*, 1760–1764.
- (15) Rullière, C.; Declémy, A. *Chem. Phys. Lett.* **1987**, *135*, 213–218.
- (16) Itoh, T. *Chem. Phys. Lett.* **1989**, *159*, 263–266.
- (17) Itoh, T.; Kohler, B. E.; Spangler, C. W. *Spectrochim. Acta, Part A* **1994**, *50*, 2261–2263.
- (18) Plakhotnik, T.; Walser, D.; Renn, A.; Wild, U. P. *Chem. Phys. Lett.* **1996**, *262*, 379–383.
- (19) Yee, W. A.; O'Neil, R. H.; Lewis, J. W.; Zhang, J. Z.; Kliger, D. S. *Chem. Phys. Lett.* **1997**, *276*, 430–434.
- (20) Walser, D.; Plakhotnik, T.; Renn, A.; Wild, U. P. *Chem. Phys. Lett.* **1997**, *270*, 16–22.
- (21) Bachilo, S. M.; Bachilo, E. V.; Gillbro, T. *Chem. Phys.* **1998**, *229*, 75–91.
- (22) Bachilo, S. M.; Spangler, C. W.; Gillbro, T. *Chem. Phys. Lett.* **1998**, *283*, 235–242.
- (23) Hirata, Y.; Mashima, K.; Fukumoto, H.; Tani, K.; Okada, T. *Chem. Phys. Lett.* **1999**, *308*, 167–180.
- (24) Yee, W. A.; O'Neil, R. H.; Lewis, J. W.; Zhang, J. Z.; Kliger, D. S. *J. Phys. Chem. A* **1999**, *103*, 2388–2393.

- (25) Renge, I. *Chem. Phys. Lett.* **2000**, *320*, 373–379.  
(26) Itoh, T. *Bull. Chem. Soc. Jpn.* **2002**, *75*, 1973–1976.  
(27) Kukura, P.; McCamant, D. W.; Davis, P. H.; Mathies, R. A. *Chem. Phys. Lett.* **2003**, *382*, 81–86.  
(28) Itoh, T. *J. Chem. Phys.* **2004**, *121*, 6956–6960.  
(29) Itoh, T. *J. Chem. Phys.* **2005**, *123*, 64302–1 – 64302–6.  
(30) Englman, E.; Jortner, J. *Mol. Phys.* **1970**, *18*, 145–164.  
(31) Bouwman, W. G.; Jones, A. C.; Phillips, D.; Thibodeau, P.; Friel, C.; Christensen, R. L. *J. Phys. Chem.* **1990**, *94*, 7429.  
(32) The location of the two-photon absorption origin of DPO is not available in the vapor phase, but it was reported to be at 22 000–23 000

$\text{cm}^{-1}$  in low-temperature matrices. It is known that the location of the  $S_1(2^1A_g)$  state is not influenced strongly by the environment. Thus, if we assume the absorption origin of 23 000  $\text{cm}^{-1}$ , then the  $\Delta E_{12}$  value estimated from the locations of the  $S_1$  and  $S_2$  absorption origins is about 5000  $\text{cm}^{-1}$  ( $= 28\,000 - 23\,000 \text{ cm}^{-1}$ ) for DPO vapor. Using the value of 5000  $\text{cm}^{-1}$  as  $\Delta E_{12}$  along with eq 1, we expect that the  $I_{F2}/I_{F1}$  value will increase by a factor of 6.0 when increasing the temperature from 98 to 136 °C. This further conflicts with the observation, indicating that most of the observed  $S_2$  fluorescence can be attributed to the prompt fluorescence.

(33) Berlman, I. B. *Handbook of Fluorescence Spectra of Aromatic Molecules*, 2nd ed.; Academic Press, New York, 1971.